

WP5: Channelling at the polycrystal scale.

Task 5.1: Polycrystalline homogenization (M1-M48)

Task leader: D. Gonçalves, CEA; other partners: JRC, METU

This task is subdivided in two sub-tasks aiming at the determination of the macroscopic tensile behaviour of irradiated F/M steels, by using mean-field and full-field homogenization approaches, respectively.

Sub-task 5.1.1: Mean-field homogenization accounting for channeling – CEA (D. Gonçalves)

A new polycrystalline homogenization model based on the formation of channel structures inside single crystals and grains, as observed experimentally for irradiated F-M steels [M. Eldrup *et al.* J. Nucl. Mater. 307-311 (2002) 912; K. Wang, Y. Dai *et al.* J. Nucl. Mater. 468 (2016) 246; S.J. Zinkle & B.N. Singh, J. Nucl. Mater. 351 (2006) 269], has been proposed by CEA. For this new model, a very small ratio between the channel thickness (about 100 nm) and the channel length (close to the grain size) leads to much lower internal stresses inside the polycrystal, yielding lower strain hardening. The model accounts for three parameters that can be measured by experimental observations (SEM, TEM, AFM, etc.): the channel thickness, the grain size and the maximum plastic slip that can be accommodated by each channel. As a first approach, intragranular hardening laws are not accounted for, and an initial critical shear stress, $\tau_{c,0}$, is considered. This material parameter is strongly dependent on the irradiation dose received by the material and its grain size. For this first approach, this parameter is the only one adjusted using the polycrystalline tensile curves.

In the elastic-plastic framework, by accounting for the increase of the number of channels with remote plastic deformation, a negligible hardening is observed. This behavior results directly from the small ratio between the channel thickness and the channel length. Moreover, the simulations predict polycrystalline tensile curves showing similar behavior as those observed for irradiated BCC iron and F-M steels. Moreover, a low number of activated slip systems is predicted, even for remote plastic strains of 10%. These predictions are in agreement with microscopic observations.

In order to avoid the use of $\tau_{c,0}$ as fitting parameter, an analytical method is proposed. The critical stress can be then defined as the sum of the Peierls stress, $\tau_{c,Peierls}$, the stress resulting from the grain size effect, $\tau_{c,HP}$, and the stress resulting from interactions between mobile dislocations and irradiation loops, $\tau_{c,loop}$. The first stress can be easily defined using tensile curves of non-irradiated single crystals. $\tau_{c,HP}$ can be defined through the Hall-Petch law. Experimentally, it has been shown that the Hall-Petch coefficient measured in the non-irradiated and irradiated materials are very similar [Kass and Murty, TMS symposium, (1996), p. 27-35]. The stress resulting from interaction between mobile dislocations and irradiation loops can be expressed using a Taylor-kind law and depends on the diameter and concentration of the irradiation loops [Monnet *et al.* J. Nuclear Mater. 541 (2019) 128]. The analytical values of $\tau_{c,0}$ determined through this method are in agreement with those fitted to polycrystalline curves.

The implementation of intragranular hardening laws is foreseen, in order to better describe the material hardening behavior under tensile tests, without using any adjusted parameter. The next step of the project consists then in predicting the tensile behavior of irradiated materials, applying experimental measurements of thickness and length of channels, carried out on irradiated Fe-9Cr (CIEMAT). The calculated curves will be then compared to the experimental ones (SCK-CEN, subtask 5.4.1), as well as to the full-field finite elements computation results (JRC, METU & CEA, subtask 5.1.2).

Sub-task 5.1.2: Full-field homogenization accounting for channeling – JRC (I. Simonovski), METU

JRC has been developing finite elements models of polycrystalline aggregates, containing 1, 2, 14 and 50 grains, where channels are explicitly built into individual grains. The grains themselves are randomly sized and shaped by using Voronoi tessellation. The crystallographic orientation of a grain is a random variable. The number of channels per grain, channel thickness and spacing (distance between the channels) are all parametrically defined, so that they can be adjusted, as suggested by CEA. These polycrystalline aggregates are then coupled with the strain gradient crystal plasticity (SGCP) model (**METU**). The introduction of explicitly built-in channels imposes severe constraints on the meshing procedure. The mesh was obtained for aggregates containing 1 (4 and 8 channels), 2 (4 channels) and 14 (4 channels) grains filled with channels. In all these cases the channel thickness $t=100$ nm and channel spacing $d=1.2$ μm has been used, with the average grain size of 23 μm . An additional procedure has been developed that allows for uniform distribution of a fixed number of channels per grain (e.g. 4), with suitably adjusted channel spacing. For the 50 grain aggregates, it was not possible to obtain error-free meshes. An automatic procedure was developed to obtain a mesh for a given grain geometry, continuously changing grain orientations (thereby changing channel orientations, as well). So far, more than 8000 different grain orientations for each of the two grain geometries have been tried, without obtaining error-free mesh.

Macroscopic responses for the single crystal (4 and 8 channels, single slip system activated and three slip systems activated) and bi-crystal (4 channels, single slip system activated) cases with explicitly built in channels have been computed. The calculations were performed with the linear hardening version of the SGCP model. The effect of the local scale factor R (radius of dislocation domain contributing to the internal stress field) on the stress and macroscopic response has been investigated:

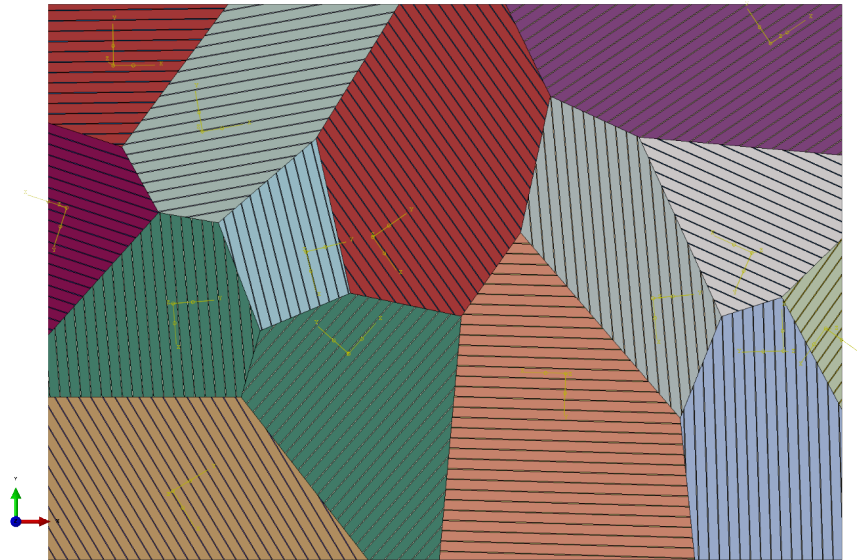
$R=0.1$ μm \rightarrow averages out stress between the channels, channels almost not visible

$R=0.05$ μm \rightarrow channels better visible in the stress field.

$R=0.025$ μm \rightarrow channels are well visible in the stress field.

Also, a 14 grain case with each grain having uniformly distributed channels was built. Calculation times were relatively short (e.g. 27500 s for 2524182 finite elements), even for the 14 grain case. The calculation time includes the CPU solver time, the conversion of the results into a post-processing readable form and the calculation of the macroscopic response.

The introduction of channels decreases the macroscopic stress. Currently, the coupling of non-linear hardening SGCP with the aggregates is under way. Although similar results can also be expected using J2 plasticity for channels and elastically deformed areas between the channels, SGCP allows the simulation of the Hall-Petch effect. Once a suitable mesh is built, the constitutive response of channels and spaces between the channels can be easily changed.



Polycrystalline aggregate with 14 grains and uniformly distributed channels

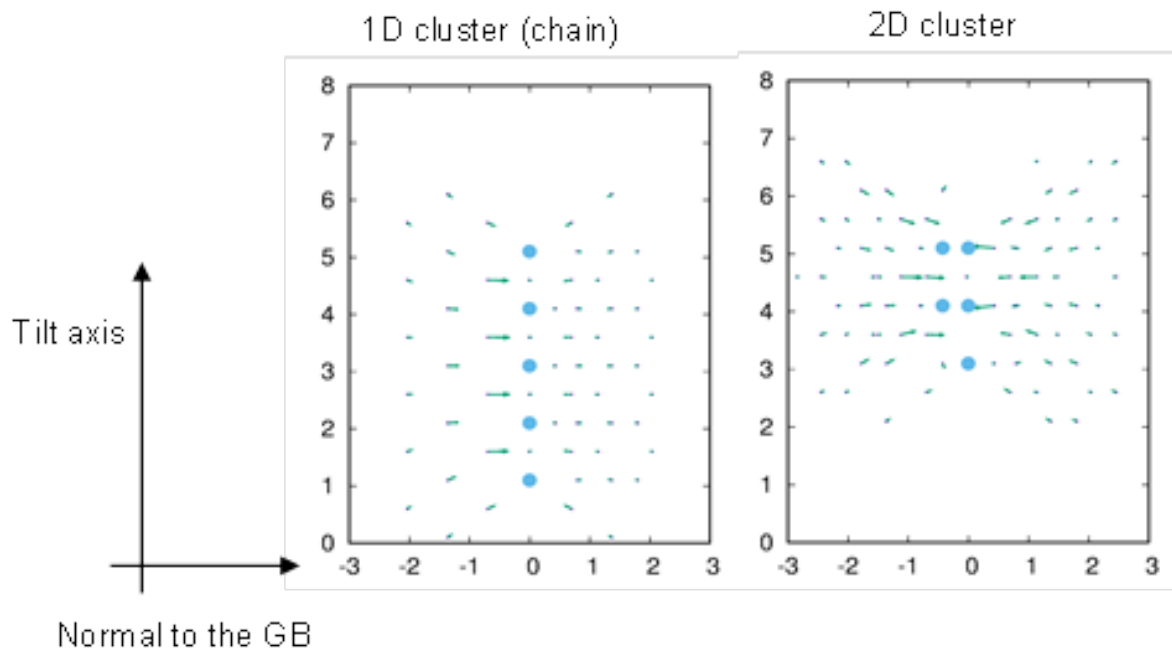
Task 5.1: Simulation of the damage initiation process during tensile loading as a consequence of channeling: Cavitation/ nano-cavitation mechanism under deformation of irradiated F/M steels (M1-M48)

Task leader: D. Tanguy, CNRS; other partners: CEA

Two cavitation scenarios are studied. The first one considers the decohesion of the carbide-matrix when approaching necking and implies an extrapolation of cavity nucleation in the un-irradiated case [B. A. Senior et al., *Acta metall.* 34 (1986) 1321-1327] towards the irradiated state (CEA, CNRS). A model is proposed where the number of voids per unit volume is a function of the thickness of the clear channel, the inter-channel spacing and the average deformation carried by one such channel (M5.2/MS19). The key constant in the model is taken from the measurement of the number of carbides broken with the average plastic deformation in TEM by Senior. In-situ high-resolution (100 nm) SEM tensile tests (CNRS), with surface field measurements, are proposed to try to observe this mechanism and measure the parameters appearing in the model (in collaboration with CIEMAT and PSI).

The second scenario is based on the clustering of vacancies, under the effect of stress concentration due to the impingement of clear channels on the grain boundaries. Indeed, in the absence of carbides, crack initiation is intergranular at necking [Y. Chen et al., *Journal of Nuclear Materials* 271&272 (1999) 128-132]. This phenomenon is studied by atomic scale simulations using an EAM potential for BCC Fe developed within the first reporting period (CNRS). Four symmetrical tilt grain boundaries were selected, two with an axis along [110] and two along [100]. Segregation energy maps for single vacancies, activation energies for single and di-vacancies, as a function of the strain perpendicular to the interface, were calculated. Segregation is strong, but tends to decrease with increasing strain. Vacancies and di-vacancies are mobile down to room temperature, with a tendency for one dimensional diffusion along the tilt axis. To go beyond di-vacancies and study clusters of larger sizes, the method call "Smart Darting" was adapted to our Metropolis Monte Carlo (MMC) code for vacancies at grain boundaries [E. Vamvakopoulos, D. Tanguy, *Phys Rev B* 79 (2009) 094116-1]. It resolves the problem of trapping of MMC when the neighbours are strongly relaxed, although at the expense of the computational cost. With this new method, clusters of vacancies of size 5 either along the tilt axis or in the form of 2D platelets were found for the $\Sigma 29(730)[001]$ grain boundary. Future work will be devoted to the study of bubbles and the comparison of their energy with respect to the platelets, in order to determine if the bubbles are

thermodynamically stable and at which strain. These conditions will be compared to the ones expected at the tip of a cleavage channel impinging on a grain boundary.



1D and 2D clusters, containing 5 vacancies, obtained by atomistic Metropolis Monte Carlo simulations in the $\Sigma 29(730)[001]$ symmetrical tilt grain boundary in bcc Fe (EAM potential M07). The circles represent the vacancies and the arrows the displacement field (the relaxation of the neighbours). The axis x and y are distances in a_0 .

Task 5.3: Development of physically based constitutive equations for describing coupled deformation damage behaviour of F/M steels (M1-M48)

Task leader: E. Gaganidze, KIT; other partners: -

This task aims at describing the coupled deformation and damage behaviour of irradiated F/M steels. It is divided into two chronologically ordered sub-tasks, i.e. the two subtasks represent the two key steps for the fulfilment of the task.

Sub-task 5.3.1: Development of physically based constitutive equations describing the deformation damage behaviour of F/M steels – KIT (E. Gaganidze)

KIT developed a physics-based continuum scale model for the description of post-yield and post-necking behaviour of irradiated F/M steels, e.g. Eurofer97. The main challenge was the identification and proposal of a suitable finite strain model enabling the description of large inelastic deformation characteristic for irradiated F/M steels. A visco-plastic model by J. Aktaa & C. Petersen (J. Nucl. Mater. 417 (2011) 1123), that is capable of describing the deformation and damage behaviour of irradiated F/M steels for small strains, is used as base model. Within the finite strain framework, the dual variables approach was chosen to formulate the large strain model. To obtain a thermodynamically consistent formulation of evolution equations for kinematic and isotropic hardening/softening, a power term was proposed and introduced into the first law of thermodynamics, to account for the energy transfer to the materials per unit time due to irradiation. Additionally, a free energy function for the elasto-plastic material was extended to describe the evolution of isotropic irradiation hardening and the kinematic hardening for finite strains. These allowed the derivation of the entropy inequality for this material and the identification of the necessary conditions to ensure thermodynamic stability.

Sub-task 5.3.2: Simulation of post-yield post-necking behaviour – KIT (E. Gaganidze)

The main focus is put on the identification of a suitable ductile damage model for accounting void nucleation and coalescence. Among the available pressure-dependent damage models, the Gurson-Trevaard-Needleman (GTN) model is the most popular, as it establishes an ellipsoid type yield surface that shrinks with the growth of the damage variable - void volume fraction (VVF) - and

provides the easy-to-implement evolution equations for determining VVF. The application of the model requires the determination of the critical void volume fraction from experiments, while the other parameters are fitted. These parameters were taken from literature [L. Stratil et al., Proc. Mat. Science 3 (2014) 1155-1160]. Alternate evolution equations to determine VVF were suggested in **M5.2** (CNRS, CEA) based on the work of Senior [B. A. Senior et al., Acta metall. 34 (1986) 1321-1327], which provides a void nucleation criterion that may be modified for application to irradiated materials. The major challenge was to extend the rate-independent plasticity-based GTN model to the rate-dependent plasticity framework. A viscoplastic potential was formulated by combining the GTN yield criteria and the viscoplastic flow rule, which was used in deriving the new flow rule and inelastic strain rate for the viscoplastic-GTN model. The model was implemented in ABAQUS for the small strain framework and the NLGEOM option was used to simulate the yielding and flow softening of irradiated Eurofer97. The results are encouraging as the desired behavior is captured. However, the model parameters at hand (used for small deformations) have to be recalibrated for a finite strain application. The finite strain model proposed in the **Sub-task 5.3.1** is under implementation in ABAQUS with the help of a complex integration algorithm capable of handling finite rotations. The model parameters will be recalibrated by using the experimental data from **Sub-task 5.4.1** (*SCK-CEN*) to replicate experimentally measured post-yielding and post-necking behaviour.

Task 5.4: Experiments to support modelling (M1-M42)

Task leader: D. Terentyev, SCK-CEN; other partners: CEA, CIEMAT

Experimental investigations to support the simulation activities carried out within the previous task will be performed in three subtasks.

Sub-task 5.4.1: Experimental validation by camera instrumented mechanical tests - SCK-CEN (D. Terentyev)

A digital image correlation procedure has been developed by **SCK-CEN** in the cold lab and then applied in hot cells to test neutron irradiated samples. The quality of the applied video registration (with fixed focus point) is sufficient to perform video recording with the furnace door closed and with the standard furnace light, which enables video-recording neutron irradiated samples during the test at elevated temperature. The video-recording can be effectively performed at the loading rate of 2 mm/min or lower. The calibration measurements were performed using non-irradiated Eurofer97 samples (from the same batch as neutron irradiation samples) in the temperature interval between RT and 300 °C. Additional tests were performed by interrupting the deformation at several points across the loading curve and high resolution photo images were taken to validate the measurements of the neck width, otherwise measured in video stream.

The neutron irradiated material used in this study is Eurofer97 grade produced by Böhler Austria GmbH (heat 83699), normalized at 979 °C for 1h 51 min followed by air cooling. The heat was tempered at 739 °C for 3h 42 min followed by air cooling. The samples were cut from the cylindrical bar such that the sample axis and bar axis coincide. The gauge diameter of the sample was 2.4 mm and length 12 mm. Several neutron irradiated samples were available for the tests committed in the M4F project. The irradiation was performed in Callisto loop in BR2 (materials testing reactor at **SCK-CEN**) at 300°C (temperature of the coolant media).

Tensile tests were performed in the temperature range of 22-300 °C. The four studied samples were irradiated to 0.22 dpa (E97-204, $T_{\text{test}}=\text{RT}$), 0.65 dpa (E97-205, $T_{\text{test}}=300\text{ °C}$), 1.05 dpa (E97-206, $T_{\text{test}}=\text{RT}$), 1.18 dpa (E97-208, $T_{\text{test}}=300\text{ °C}$). The resulting engineering and true stress – engineering strain curves are deduced from the experimentally measured load-displacement. The samples irradiated to a dose higher than 0.65 dpa show very low uniform elongation and deform by early necking. Based on the derivation of the neck cross-section by video registration (with automatic

cross-section calculation), the true stress was recalculated. The Bridgman correction was then applied by extracting snapshots from the video streams, and the comparison of the corrected stress with engineering as well as true stress (from video). From the obtained results, it follows that only the 1.18 dpa irradiated sample shows the decrease of the true stress after the yield (i.e. strain softening phenomena), which is also seen on the engineering stress-strain curve (as an inflection point). For samples tested at 300 °C, the fracture occurs when the true stress reaches ~0.8-0.85 GPa, while for those tested at RT, the fracture occurs at ~1 GPa.

Sub-task 5.4.2: TEM examination of irradiated and deformed materials - CIEMAT (M. H. Mayoral), SCK-CEN

Localized deformation in neutron irradiated Eurofer97 will be investigated by TEM after tensile testing at **SCK-CEN**. All mechanical tests have been performed. The fracture surface is analyzed. The activity on the surface of the fractured samples was also measured, which enabled the deployment of the samples to the FIB. The FIB sessions have been performed in July 2020 to fabricate several TEM samples (from different locations of the sample within the necking area). TEM examinations of the FIB-cut lamellas have been carried out. The analysis of the TEM results is underway.

Localized deformation in ion and proton irradiated: TEM in-situ strained specimens will be investigated by means of TEM at **CIEMAT**. The fully ferritic alloy Fe-9Cr has been chosen for irradiation with ions and protons at HZDR and CNRS/CEMTHI in collaboration with PSI. Ion irradiation experiments have been performed in January 2019 at HZDR, and proton irradiations have been performed in April 2020 at CNRS/CEMHTI & PSI as part of **WP2**. After in-situ straining experiments at CIEMAT (RT) within **WP4**, the deformed samples will be characterized by TEM by **CIEMAT** as part of this WP, in order to provide quantitative information of the pre-irradiated and deformed microstructure. This work will start after the analysis by SEM-EBSD is performed in **Sub-task 5.4.3**.

Sub-task 5.4.3: AFM and SEM-FEG study of surfaces of irradiated and deformed specimens – CEA (C. Robertson), CIEMAT

The present work at **CEA** is closely related to **Task 4.4** and **Sub-task 4.3.2**. Strained specimens are examined using AFM technique, yielding reference surface marking displacements in several selected grains. This quantitative evaluation is carried out and compared with its theoretical counterpart in as-received, un-irradiated material conditions (cf. **Sub-task 4.3.2**). A ferritic model material (16MND5 bainitic low carbon steel) having a grain/lath microstructure nearly identical to Eurofer97 steel is strained up to $\gamma = 7-10\%$ at 77 K. In these conditions, the theoretical inter-band spacing $d = 0.4-0.7 \mu\text{m}$ and surface marking displacement $h = 40-60 \text{ nm}$. AFM measurements yield $h = 10-70 \text{ nm}$ depending on the deformed grain considered. Further step height evaluations will be carried out on ion-irradiated materials during the upcoming period, depending on available results/specimens.

In combination with **Sub-task 5.4.2** and Tasks in **WP4**, after in-situ straining experiments, the deformed samples will be characterized by SEM-EBSD at **CIEMAT** in order to provide information about deformation modes on pre-irradiated and deformed samples. Samples already strained at in-situ experiments performed by CNRS/CEMES are already at **CIEMAT** and SEM-EBSD examination will start by September 2020. Additionally, selected samples will be examined by AFM by **CEA** for the evaluation of surface steps and then plastic slips carried out by clear bands.